Deposition under Turbulent Flow of Wax−Solvent Mixtures in a Bench-Scale Flow-Loop Apparatus with Heat Transfer†

ARTICLE *in* ENERGY & FUELS · DECEMBER 2006

Impact Factor: 2.79 · DOI: 10.1021/ef0603784

2 AUTHORS, INCLUDING:

Anil K Mehrotra
The University of Calgary
160 PUBLICATIONS **2,348** CITATIONS

SEE PROFILE

Deposition under Turbulent Flow of Wax−Solvent Mixtures in a Bench-Scale Flow-Loop Apparatus with Heat Transfer†

Nelson Fong and Anil K. Mehrotra*

Department of Chemical and Petroleum Engineering, University of Calgary, Calgary, Alberta, Canada T2N 1N4

Received August 14, 2006. Revised Manuscript Received October 28, 2006

A flow-loop apparatus, incorporating a co-current double-pipe heat exchanger, was developed for investigating the deposition of solids from solutions of a multicomponent wax in a paraffinic solvent under turbulent flow. The deposition experiments were performed at Reynolds numbers of 10 000−31 000 with 7, 10, and 15 mass % wax−solvent mixtures at different hot and cold stream temperatures. In all experiments, the deposit was formed rapidly such that a thermal steady state was attained within 20−30 min. The deposit mass decreased with an increase in the Reynolds number, the wax−solvent mixture temperature, and the coolant temperature. The data were analyzed with a steady-state heat-transfer model, which confirmed the deposit mass to depend upon the relative magnitudes of the thermal resistances in series as well as the fractional temperature drop across the deposit layer. The estimated liquid−deposit interface temperature was shown to be close to the wax appearance temperature of each wax−solvent mixture. The average thermal conductivity of the deposit was estimated to be 0.35 W m^{-1} K^{-1}. The gas chromatograph analysis of deposit samples showed their wax content and carbon-number distribution to vary with the deposition time and Reynolds number. Overall, the results of this study confirm that the deposition process from "waxy" mixtures is primarily thermally driven under both laminar and turbulent flow.

Introduction

Many crude oils contain substantial fractions of petroleum wax, which is a major constituent of "waxy" deposits from crude oils. When a "waxy" crude oil, comprised of high-molecular-weight paraffins, flowing through a pipeline is exposed to a cold environment that is below its solubility temperature, solids deposition on the pipe wall is known to occur. The adverse effects of such deposition are encountered in production, transportation, and processing operations of the petroleum industry, including the blockage of pipelines and equipment, which require expensive remediation techniques involving mechanical or chemical cleaning.

The highest temperature at which the first crystals of paraffin wax start to appear upon cooling of paraffinic mixtures, such as "waxy" crude oils, is called the wax appearance temperature (WAT). Wax molecules crystallize out of the liquid mixture when its temperature falls below the WAT, which may lead eventually to their deposition on the pipe wall. The precipitation and deposition of wax crystals are two different but related processes; wax precipitation is governed primarily by thermodynamic considerations, whereas wax deposition is predominantly a transport process, which requires a thermal gradient. For example, Bidmus and Mehrotra[1] found no deposition in the absence of a thermal driving force, even though wax crystals were present in the mixture held at a temperature below the WAT. Bhat and Mehrotra[2] pointed out the difference between the WAT and the wax disappearance temperature (WDT). The WAT is measured during cooling of the sample, while the WDT is recorded during heating. It was shown that the WDT, rather than the WAT, is closer to the thermodynamic liquidus (or saturation) temperature of wax−solvent mixtures.[2]

Holder and Winkler[3] studied wax deposits using cross-polarized microscopy and reported that the crystallites have structures of platelets that overlap and interlock. The wax−oil gel is formed as a result of the flocculation of orthorhombic wax crystallites that appear in the solution during cooling.[4] A solid network structure is formed when sufficient quantities of paraffin crystals are formed, which leads to the formation of a gel-like structure with entrapped liquid oil. That is, wax deposits consist of two phases: liquid oil and solid wax. Upon cooling below the pour point temperature (PPT), "waxy" mixtures and crude oils show complex non-Newtonian thixotropic behavior with a considerable increase in the apparent viscosity.[5−7]

† Presented at the 7th International Conference on Petroleum Phase Behavior and Fouling.

* To whom correspondence should be addressed. Telephone: (403) 220-7406. Fax: (403) 284-4852. E-mail: mehrotra@ucalgary.ca.

(1) Bidmus, H. O.; Mehrotra, A. K. Heat-Transfer Analogy for Wax Deposition from Paraffinic Mixtures. *Ind. Eng. Chem. Res.* **2004**, *43*, 791.

(2) Bhat, N. V.; Mehrotra, A. K. Measurement and Prediction of the Phase Behavior of Wax−Solvent Mixtures: Significance of the Wax *Dis*appearance Temperature. *Ind. Eng. Chem. Res.* **2004**, *43*, 3451.

(3) Holder, G. A.; Winkler, J. Wax Crystallization from Distillate Fuels. I. Cloud and Pour Phenomena Exhibited by Solutions of Binary *n*-Paraffin Mixtures. *J. Inst. Petrol.* **1965**, *51*, 228.

(4) Dirand, M.; Chevallier, V.; Provost, E.; Bouroukba, M.; Petitjean, D. Multicomponent Paraffin Waxes and Petroleum Solid Deposits: Structural and Thermodynamic State. *Fuel* **1998**, *77*, 1253.

(5) Wardhaugh, L. T.; Boger, D. V. Measurement of the Unique Flow Properties of Waxy Crude Oils. *Chem. Eng. Res. Des.* **1987**, *65*, 74.

(6) Rønningsen, H. P.; Bjørndal, B.; Hansen, A. B.; Pedersen, W. B. Wax Precipitation from North Sea Crude Oil: Crystallization and Dissolution Temperatures, and Newtonian and Non-Newtonian Flow Properties, *Energy Fuels* **1991**, *5*, 895.

(7) Tiwary, D.; Mehrotra, A. K. Phase Transformation and Rheological Behaviour of Highly Paraffinic "Waxy" Mixtures. *Can. J. Chem. Eng.* **2004**, *82*, 162.

10.1021/ef0603784 CCC: $37.00
Published on Web 12/15/2006

The process of deposit formation from "waxy" mixtures or crude oils is a complex problem, which may involve several considerations, such as solid−liquid multiphase equilibria, crystallization kinetics, fluid dynamics, heat transfer, mass transfer, rheology, and thermophysical and transport properties. The liquid−solid-phase ratio as well as the deposit composition have been reported to change with time through a process referred to as "deposit aging",[1,8−13] which may be attributed to diffusion within the deposit, interphase mass transfer, and/or the effect of shear stress caused by the flowing crude oil on the deposit layer.

Several mechanisms have been proposed for the formation of deposits from "waxy" mixtures and crude oils.[14] Of these, the approach involving molecular diffusion as the predominant mechanism for solids deposition from waxy oils has been employed in a number of studies.[8,15−22] This diffusion-driven approach for deposit formation is based on the premise that the flow of "waxy" crude oils in a pipeline, whose wall temperature is below the WAT, provides a radial temperature gradient, which creates a concentration gradient for molecular diffusion in the radial direction. The rate of mass transfer at the liquid−deposit interface is equated at every time interval to obtain the deposition amount, and an energy balance is used to back-calculate the liquid−deposit interface temperature (denoted here by T_d). The underlying pseudo-steady-state assumption gives rise to a gradual increase in T_d, during the deposition process, from an initial value close to the wall temperature (<WAT).

An alternate approach considers the important role of heat transfer in the formation and growth of deposits, and it has also been investigated directly or indirectly in several studies.[1,13,18,23−30] Of particular relevance to this study is the heat-transfer analogy, proposed by Bidmus and Mehrotra[1] and Parthasarathi and Mehrotra,[13] that yielded good agreement with the experimental results for the deposition of solids from wax−solvent mixtures under laminar flow. From a large number of heat-transfer experiments under laminar flow,[1,13] it was shown that (a) the deposit-layer formation takes place in a relatively short time of less than 30 min, (b) the concentration of heavier paraffins in the deposit layer increases only slightly with time, (c) the steady-state liquid−deposit interface temperature, T_d, is equal to the WAT of each wax−solvent mixture, (d) the deposit mass depends upon the individual temperature difference across each of the thermal resistances and not the overall temperature difference, and (e) the average deposit thermal conductivity is about 0.22−0.30 W m^{-1} K^{-1}. A dimensionless parameter, θ_d, was defined as the ratio of the temperature drop across the deposit layer and the overall temperature difference, and it was related to the deposit mass.[1] It was shown that, at a steady state, θ_d is also equal to the ratio of the deposit-layer thermal resistance and the sum of all of thermal resistances.

This study extends the laminar flow deposition studies[1,13] into the turbulent flow regime. A bench-scale flow-loop apparatus, similar to that of Parthasarathi and Mehrotra,[13] was developed for much higher flow rates corresponding to a Reynolds number of 10 000−31 000. A design of experiments was implemented to study the deposition of solids from prepared multicomponent wax−solvent mixtures of known composition. The experimental program investigated the effects of the wax concentration, wax−solvent solution temperature (above its WAT), coolant temperature (below the WAT), and Reynolds number (or shear rate). Because all experiments were performed with the wax−solvent solution temperature above the corresponding WAT, the liquid phase did not contain any solid phase. In addition, extended deposition experiments, lasting up to 8 h, were performed to study the effect of the deposition time on deposit properties. The gas chromatograph (GC) analyses of deposit samples were used to interpret the changes in deposit composition. The results of this study provide further confirmation that the deposition process is predominantly a thermally driven process.

Heat-Transfer Considerations

Consider the cooling of a "hot" wax−solvent mixture at a temperature higher than its WAT, i.e., T_h > WAT, flowing through a pipe, by a coolant at a temperature below its WAT, i.e., T_c < WAT. Heat transfer from the wax−solvent mixture to the coolant results in a radial temperature gradient, which would lead to the formation of a deposit layer, provided that the inside tube-wall temperature, T_{wi}, is less than the WAT. The deposit layer would offer additional thermal resistance to the transfer of thermal energy from the wax−solvent mixture

(8) Singh, P.; Venkatesan, R.; Fogler, H. S.; Nagarajan, N. Formation and Aging of Incipient Thin Film Wax−Oil Gels. *AIChE J.* **2000**, *46*, 1059.
(9) Singh, P.; Venkatesan, R.; Fogler, H. S.; Nagarajan, N. Morphological Evolution of Thick Wax Deposits during Aging. *AIChE J.* **2001**, *47*, 6.
(10) Singh, P.; Youyen, A.; Fogler, H. S. Existence of a Critical Carbon Number in the Aging of a Wax−Oil Gel. *AIChE J.* **2001**, *47*, 2111.
(11) Coutinho, J. A. P.; Lopes da Silva, J. A.; Ferreira, A.; Soares, M. R.; Daridon, J. L. Evidence for the Aging of Wax Deposits in Crude Oils by Ostwald Ripening. *Pet. Sci. Technol.* **2003**, *21*, 381.
(12) Paso, K. G.; Fogler, H. S. Influence of *n*-Paraffin Composition on the Aging of Wax−Oil Gel Deposits. *AIChE J.* **2003**, *49*, 3241.
(13) Parthasarathi, P.; Mehrotra, A. K. Solids Deposition from Multicomponent Wax−Solvent Mixtures in a Benchscale Flow-Loop Apparatus with Heat Transfer. *Energy Fuels* **2005**, *19*, 1387.
(14) Azevedo, L. F. A.; Teixeira, A. M. A Critical Review of the Modeling of Wax Deposition Mechanisms. *Pet. Sci. Technol.* **2003**, *21*, 393.
(15) Majeed, A.; Bringedai, B.; Overa, S. Model Calculates Wax Deposition for N. Sea Oils. *Oil Gas J.* **1990**, *18*, 63.
(16) Svendsen, J. A. Mathematical Modeling of Wax Deposition in Oil Pipeline Systems. *AIChE J.* **1993**, *39*, 1377.
(17) Hsu, J. J. C.; Brubaker, J. P. Wax Deposition and Scale-Up Modeling for Waxy Live Crudes under Turbulent Flow Conditions. Presented at the SPE International Meeting, Beijing, China, Nov 14−17, 1995; SPE paper 29976.
(18) Creek, J. L.; Lund, H. J.; Brill, J. P.; Volk, M. Wax Deposition in Single Phase Flow. *Fluid Phase Equilib.* **1999**, *801*, 158−160.
(19) Singh, P.; Venkatesan, R.; Fogler, H. S.; Nagarajan, N. Prediction of the Wax Content of the Incipient Wax−Oil Gel in a Pipeline: An Application of the Controlled Stress Rheometer. *J. Rheol.* **1999**, *43*, 1437.
(20) Kok, M. V.; Saracoglu, R. O. Mathematical Modeling of Wax Deposition in Crude Oil Pipelines (Comparative Study). *Pet. Sci. Technol.* **2000**, *18*, 1121.
(21) Ramirez-Jaramillo, E.; Lira-Galeana, C.; Brito, O. M. Numerical Model for Wax Deposition in Oil Wells. *Pet. Sci. Technol.* **2001**, *19*, 587.
(22) Ramirez-Jaramillo, E.; Lira-Galeana, C.; Manero, O. Modeling Wax Deposition in Pipelines. *Pet. Sci. Tehcnol.* **2004**, *22*, 821.
(23) Cole, R. J.; Jennsen, F. W. Paraffin Deposition. *Oil Gas J.* **1960**, *58*, 87.
(24) Patton, C. C.; Casad, B. M. Paraffin Deposition from Refined Wax−Solvent Systems. *Soc. Pet. Eng. J.* **1970**, *10*, 17.
(25) Bott, T. R.; Gudmunsson, J. S. Deposition of Paraffin Wax from Kerosene in Cooled Heat Exchanger Tubes. *Can. J. Chem. Eng.* **1977**, *55*, 381.
(26) Mehrotra, A. K. Comments on: Wax Deposition of Bombay High Crude Oil under Flowing Conditions. *Fuel* **1990**, *69*, 1575.
(27) Ghedamu, M.; Watkinson, A. P.; Epstein, N. Mitigation of Wax Buildup on Cooled Surfaces. In *Fouling Mitigation of Industrial Heat-Exchange Equipment*; Panchal, C. B., Bott, T. R., Somerscales, E. F. C., Toyama, S., Eds.; Begell House: New York, 1997; pp 473−489.
(28) Wu, C.; Wang, K.-S.; Shuler, P. J.; Tand, Y.; Creek, J. L.; Carlson, R. M.; Cheung, S. Measurement of Wax Deposition in Paraffin Solutions. *AIChE J.* **2002**, *48*, 2107.
(29) Mehrotra, A. K.; Bidmus, H. O. Heat-Transfer Calculations for Predicting Solids Deposition in Pipeline Transportation of "Waxy" Crude Oils. In *Heat Transfer Calculations*; Kutz, M., Ed.; McGraw-Hill: New York, 2005; Chapter 25.
(30) Bhat, N. V.; Mehrotra, A. K. Modeling of Deposit Formation from "Waxy" Mixtures via Moving Boundary Formulation: Radial Heat Transfer under Static and Laminar Flow Conditions. *Ind. Eng. Chem. Res.* **2005**, *44*, 6948.

to the coolant, which would decrease the rate of heat transfer. The deposit layer would grow in thickness until attaining a thermal steady state, at which point the deposit-layer thermal resistance as well as all other resistances will become constant. In addition, the rates of heat transfer across the wax−solvent mixture, the deposit layer, the tube wall, and the coolant will become the same at the thermal steady state.

For the double-pipe heat exchanger used co-currently for deposition in the flow-loop apparatus, the rate of thermal energy released by the wax−solvent mixture and the rate of thermal energy accepted by the coolant are equal to the rate of heat transfer at the steady state, as follows:

$$q = \dot{m}_h C_h (T_{hi} - T_{ho}) = \dot{m}_c C_c (T_{co} - T_{ci}) - q_{gain} = U_i A_i \frac{[(T_{hi} - T_{ci}) - (T_{ho} - T_{co})]}{\ln[(T_{hi} - T_{ci})/(T_{ho} - T_{co})]} \quad (1)$$

The combined thermal resistance is the sum of four individual thermal resistances in series, i.e.,

$$\frac{1}{U_i A_i} = \frac{1}{2\pi(r_i - x_d)Lh_h} + \frac{\ln(r_i/(r_i - x_d))}{2\pi k_d L} + \frac{\ln(r_o/r_i)}{2\pi k_m L} + \frac{1}{2\pi r_o L h_c} \quad (2)$$

When the heat flux is equated through each of the four thermal resistances included in U_i, we obtain

$$\frac{q}{A_i} = \frac{h_h(T_h - T_d)}{r_i/(r_i - x_d)} = \frac{k_d(T_d - T_{wi})}{r_i \ln(r_i/(r_i - x_d))} = \frac{k_m(T_{wi} - T_{wo})}{r_i \ln(r_o/r_i)} = \frac{h_c(T_{wo} - T_c)}{r_i/r_o} \quad (3)$$

where x_d is the average deposit-layer thickness, k_d is the average deposit thermal conductivity, T_d is the liquid−deposit interface temperature, T_h is the average temperature of the wax−solvent mixture, and T_c is the average temperature of the coolant. Using experimental data for q, A_i, T_h, T_c, h_h, h_c, r_i, r_o, x_d, and k_m, the four equalities in eq 3 can be solved simultaneously to obtain T_{wi}, T_{wo}, T_d, and k_d. These unknowns include the two important quantities of interest, i.e., T_d and k_d.

When the expressions for the steady-state rate of heat transfer across the deposit layer and the overall rate of heat transfer were equated, Bidmus and Mehrotra[1] proposed a dimensionless ratio, θ_d, which is the ratio of the deposit-layer thermal resistance to the combined thermal resistance. Note that θ_d represents the fractional thermal resistance offered by the deposit layer, and it is also equal to the ratio of the temperature drop across the deposit layer to the overall thermal driving force. That is,

$$\theta_d \equiv \frac{R_d}{R_h + R_d + R_m + R_c} = \frac{T_d - T_{wi}}{T_h - T_c} \quad (4)$$

where $R_h = [2\pi(r_i - x_d)Lh_h]^{-1}$, $R_d = [(2\pi Lk_d)/\ln\{r_i/(r_i - x_d)\}]^{-1}$, $R_m = [(2\pi Lk_m)/\ln\{r_o/r_i\}]^{-1}$, and $R_c = [2\pi r_o L h_c]^{-1}$. Similar ratios for the other three thermal resistances are

$$\theta_h \equiv \frac{R_h}{R_h + R_d + R_m + R_c} = \frac{T_h - T_d}{T_h - T_c} \quad (5)$$

$$\theta_m \equiv \frac{R_m}{R_h + R_d + R_m + R_c} = \frac{T_{wi} - T_{wo}}{T_h - T_c} \quad (6)$$

$$\theta_c \equiv \frac{R_c}{R_h + R_d + R_m + R_c} = \frac{T_{wo} - T_c}{T_h - T_c} \quad (7)$$

For typical experimental conditions with the 7 mass % wax−solvent mixture under turbulent flow in this study, calculations were performed to predict the effect of the deposit-layer thickness on θ_h, θ_d, θ_m, and θ_c. The predicted effects of the deposit-layer thickness (relative to the inside tube radius), x_d/r_i, on the fractional thermal resistances are shown in Figure 1. Note that the predictions at Re = 10 000 are shown as the lighter curves in Figure 1 and those at Re = 30 000 are shown as the darker curves. At Re = 10 000, the deposit layer offers the dominant thermal resistance when $x_d/r_i > 0.02$. At Re = 30 000, because of an increased h_h (or a lower R_h), the deposit layer is predicted to offer the dominant thermal resistance when x_d exceeds only about 1% of r_i. Interestingly, at Re = 30 000, the two predicted convective resistances offer about the same fractional thermal resistance for all deposit-layer thicknesses. For the 10 and 15 mass % wax−solvent mixtures under turbulent flow, the predicted trends were similar to those in Figure 1.[31]

Experimental Section

Materials. All of the deposition experiments were performed with prepared multicomponent wax−solvent mixtures. Thus, the results from this study could be compared to two similar deposition studies under laminar flow of the prepared wax−solvent mixtures.[1,13] The results from these investigations could be validated, in future, with crude oil samples.

The wax, Parowax, used in this study was obtained from Conros Corporation (Scarborough, Ontario, Canada) in the form of small granules. It was different from the Aldrich wax used in the previous studies.[1,2,13] This wax was comprised of hydrocarbons in the range of C_{19}−C_{60}. Its melting point and density (at 23 °C) were measured as 57−62 °C and 915 kg m^{-3}, respectively. The solvent used for preparing wax−solvent mixtures was Norpar13, obtained from Imperial Oil (Canada), and it was comprised of *n*-alkanes ranging from C_{10} to C_{16}. Norpar13 has a density of 754 kg m^{-3} at 23 °C.

Each 9 L batch of wax−solvent mixtures was prepared by mixing preweighed amounts of Parowax and Norpar13 to obtain the desired composition. Note that the 9 L batch size was large enough such that the deposition in each experiment was not affected by a depletion of C_{20}^+ constituents in the wax−solvent mixture.[31] The mixture was heated and stirred until all of the wax had dissolved, resulting in a clear solution.

GC Analyses. All gas chromatographic analyses were performed using a HP6890 GC equipped with a nonpolar fused-silica column (10 m × 0.53 mm × 0.88 μm) and a hydrogen flame ionization detector (FID). The GC was calibrated using the ASTM D2887 extended method, using a C_5−C_{66} *n*-alkanes standard obtained from Separation Systems, Inc. (Gulf Breeze, FL). All GC analyses indicated trace amounts (<0.05 mass %) of C_{51}−C_{60} such that their combined mass fraction accounted for less than 0.2 mass % of wax;[31] hence, all GC analyses were normalized by neglecting the C_{51}−C_{60} fractions.

Figure 2 shows the carbon-number distribution of Norpar13 and Parowax. Also plotted for a comparison is the carbon-number distribution of Aldrich wax used in previous studies.[1,2,13] The main constituents in Norpar13 are C_{13} and C_{14}, with concentrations of 51.3 and 32.8 mass %, respectively. The average molar mass of Norpar13 is 185.7 kg kmol^{-1}, which corresponds to a carbon number of about 13. Parowax shows a broader distribution, compared to Aldrich wax, with C_{26}, C_{27}, C_{28}, and C_{29} being the main constituents at concentrations of 8.6, 10.1, 8.8, and 9.1 mass %, respectively. The average molar mass of Parowax was estimated

(31) Fong, N. An Experimental Investigation of Deposition From Wax−Solvent Mixtures under Turbulent Flow with Heat Transfer. M.Sc. Thesis, University of Calgary, Calgary, Alberta, Canada, 2006.

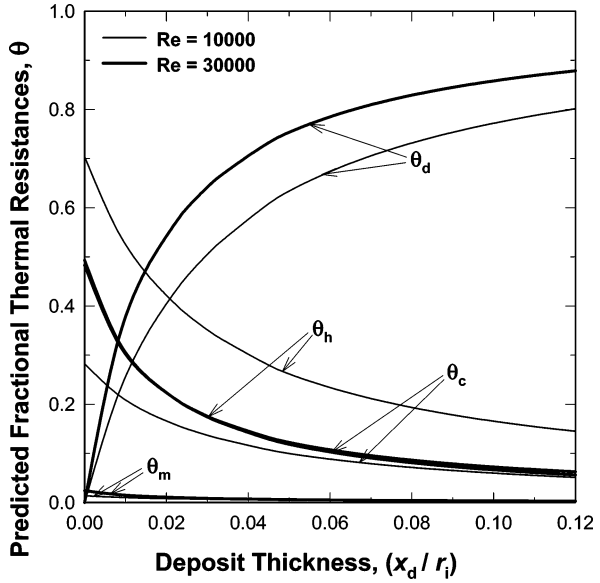

Figure 1. Predicted effects of the deposit-layer thickness on fractional thermal resistances [7 mass % wax−solvent mixture, with $k_d = 0.35$ W m^{-1} K^{-1}, at Re = 10 000 and 30 000].

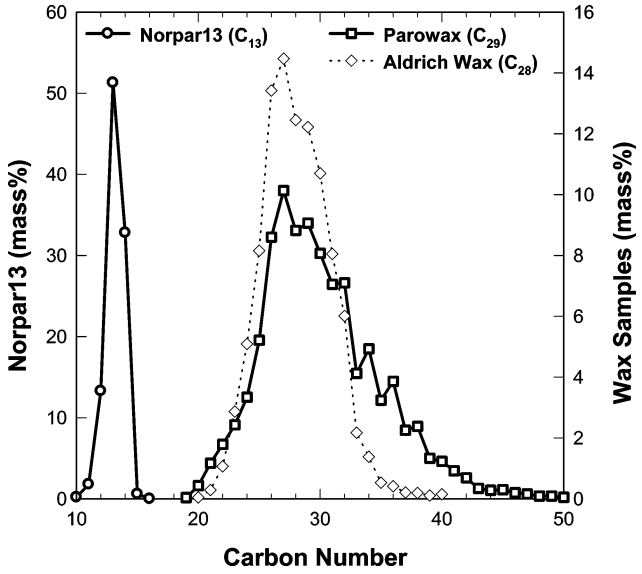

Figure 2. GC analyses for the carbon-number distribution of Parowax (wax) and Norpar13 (solvent).

to be 414.2 kg kmol^{-1}, which corresponds to a carbon number of about 29, which is also the median carbon number. It is important to note that, in Figure 2, there is no overlap in the carbon-number distributions of Parowax and Norpar13, which, as shown later, is an important requirement for interpreting the compositional changes in the deposit samples (on a solvent-free basis).

WAT Measurements. The WAT and the PPT of seven prepared wax−solvent mixtures, ranging from 5 to 20 mass % Parowax, were measured at atmospheric pressure using a visual method with cooling in steps of 1 °C.[7] The results are plotted in Figure 3 and compared with the reported WAT data for mixtures of Aldrich wax and Norpar13.[2] The error bars in Figure 3 indicate that the actual WAT could be between the reported WAT and WAT + 1 °C. As expected, the PPT of each Parowax−Norpar13 mixture is less than its WAT; however, the difference between WAT and PPT is not the same at all wax concentrations. The PPT data show a sharp decline at wax concentrations below about 10 mass %.

The WAT for Parowax−Norpar13 mixtures varied from 34 °C for 5 mass % to 43 °C for 20 mass %. For similar mixtures of Aldrich wax and Norpar13, the reported range of WAT was from 23 to 35 °C.[2] The difference in the two sets of WAT values is

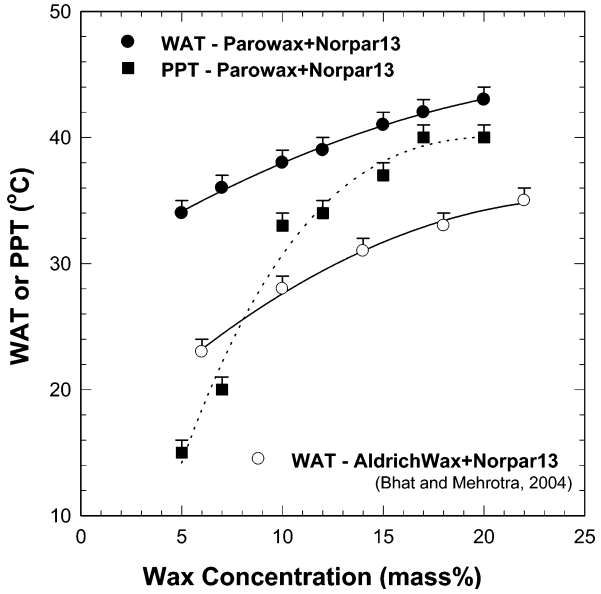

Figure 3. WAT and PPT of wax−Norpar13 mixtures.

attributed to Parowax containing a larger fraction of heavier *n*-alkanes than Aldrich wax, as shown in Figure 2.

Viscosity, Density, and Specific Heat Capacity of Parowax−Norpar13 Mixtures. These properties were needed in the heat-transfer calculations as well as for estimating the Reynolds number and mass flow rate of the wax−solvent mixtures. A calibrated Canon−Fenske viscometer (Cole−Parmer, size 50) was used for measuring the kinematic viscosities of 7, 10, and 15 mass % solutions as well as Norpar13 at several temperatures ranging from their respective WAT to about 60 °C. The density of each solution was measured using a 25 mL glass pycnometer at several temperatures ranging from their WAT to about WAT + 15 °C. The average specific heat capacity of each Parowax−Norpar13 mixture, C_h, was calculated as the weighted average of the heat capacities of components in the mixture.[30] The component specific heat capacities were estimated from a group contribution method developed by Jin and Wunderlich.[32] The viscosity (μ, in units of Pa s), density (ρ, in units of kg m^{-3}), and specific heat capacity (C_h, in units of J kg^{-1} K^{-1}) data for each Parowax−Norpar13 mixture were fitted (with $R^2 > 0.99$ in each case) to the following correlations that were used for interpolation:

$$\mu = 10^{-3} \times \exp[a_1 + a_2/(T_h + 273.15)] \quad (8)$$

$$\rho = b_1 + b_2 T_h \quad (9)$$

$$C_h = c_1 + c_2 T_h \quad (10)$$

Regression constants a_1 and a_2, b_1 and b_2, and c_1 and c_2 in eqs 8−10, respectively, are listed in Table 1.

Flow-Loop Apparatus for Heat-Transfer Deposition Experiments. A bench-scale flow-loop apparatus was designed to conduct deposition experiments under the turbulent flow regime. The apparatus is shown schematically in Figure 4. The flow-loop consisted of a double-pipe heat exchanger, a temperature-regulated heating bath holding a 10 L reservoir with a WA-1 hydromatic submersible pump (Western Pump, Calgary, Alberta, Canada) for recirculating the wax−solvent mixture, a temperature-regulated refrigerated bath with a centrifugal pump for circulating the coolant (water), a flowmeter, a valve for regulating the flow of wax−solvent mixtures, and thermocouples connected to a data-logger. The various components were interconnected with copper pipes, Tygon tubes, and hydrocarbon-resistant tubes, and all of the exposed

(32) Jin, Y.; Wunderlich, B. Heat Capacities of Paraffins and Polyethylene. *J. Phys. Chem.* **1991**, *95*, 9000.

Table 1. Constants in Eqs 8−10; Correlations for Viscosity, Density, and Specific Heat Capacity of the Solutions of Parowax in Norpar13 (Applicable at Temperatures Higher than the Respective WAT)

	constants in the viscosity correlation, eq 8		constants in the density correlation, eq 9		constants in the specific heat capacity correlation, eq 10[a]	
wax concentration	a_1	a_2	b_1	b_2	c_1	c_2
0 mass %	-5.02 ± 0.05	1710 ± 15	769.1 ± 0.9	-0.650 ± 0.018	2379	1.370
7 mass %	-4.50 ± 0.07	1580 ± 21	772.9 ± 0.6	-0.673 ± 0.013	2382	1.361
10 mass %	-4.75 ± 0.08	1720 ± 27	772.6 ± 1.2	-0.623 ± 0.024	2383	1.356
15 mass %	-4.53 ± 0.08	1610 ± 25	777.8 ± 0.8	-0.664 ± 0.015	2385	1.347

[a] Estimated.[32]

surfaces were adequately insulated. An insulated straight copper tube (2.54 cm i.d. and 57 cm long) was used before the wax−solvent mixture entered the heat exchanger.

The deposition took place on the inner surface of a machined aluminum tube, 2.54 cm (i.d.) × 3.30 cm (o.d.) × 10.16 cm (long), which formed the inner tube of the double-pipe heat exchanger. The outer tube of the heat exchanger was made of plexiglass, 3.80 cm (i.d.) × 4.60 cm (o.d.) × 10.16 cm (long). The outside surface of the plexiglass tube was insulated with 2-cm-thick styrofoam insulation to minimize the heat exchange (q_{gain}) with the surroundings. An air vent was provided at the outlet of the deposition section to allow for rapid draining of the wax−solvent mixture at the termination of each run. The paddle-wheel-type flowmeter, with a range of 0.25−2.5 L/s and connected to a Florite 700 ratemeter (Proteus Industries, Mountainview, CA), was placed at the outlet end of the heat exchanger. The coolant (water) was circulated cocurrently through the annulus of the heat exchanger at a constant rate of 0.0259 L/s.

Calibrated T-type thermocouples were used to measure the inlet temperature of the wax−solvent mixture (T_{hi}), the inlet coolant temperature (T_{ci}), and the outlet coolant temperature (T_{co}). The outlet wax−solvent mixture temperature (T_{ho}) could not be measured reliably; hence, it was estimated from the energy balance given by eq 1. From heat-transfer calculations, q_{gain} was estimated to be less than 1% of the overall rate of heat transfer, q.[31] Further details of the apparatus and calibration procedure have been reported by Fong.[31]

Procedure for Deposition Experiments. The flow loop was assembled, and the 10 L reservoir was filled with the wax−solvent mixture. After the desired heating and cooling bath temperatures were attained, the submersible pump was turned on. The flow-regulating valve was adjusted to achieve the desired flow rate. The deposition process was commenced by circulating the coolant (water) at a flow rate of 0.0259 L/s, from the refrigerated bath, through the annular side of the heat exchanger. During each deposition experiment, the readings of T_{hi}, T_{ci}, and T_{co} as well as the wax−solvent mixture flow rate were recorded using the datalogger.

The deposition experiment was terminated by stopping the submersible pump followed by quickly draining the wax−solvent mixture from the heat exchanger (by opening the air-vent valve). In preliminary experiments, it was noted that a delay of even a few seconds in the draining step caused additional deposition, which was observed to be formed as a large streak, shaped like a "speed bump", along the bottom inner surface of the aluminum tube.[31] The addition of the air vent as well as an upward inclination of the heat-exchanger assembly, as shown in Figure 4, greatly improved the draining process, but a small "speed bump" was still evident, as shown in the photographs in Figure 5. The coolant circulation was discontinued and, after the coolant was drained, the heat exchanger was dismantled to carefully recover the aluminum tube. The aluminum tube with the deposit was weighed on an electronic balance to ±0.1 mg, and the deposit mass was obtained by the difference. A sample of the deposit (and the wax−solvent mixture) was saved for GC analysis, and the remainder was recycled into the wax−solvent mixture reservoir for subsequent deposition experiments. This deposit recycling allowed for the composition of the wax−solvent mixture to not change significantly between runs. Each 9 L batch of the wax−solvent mixture was used only for 15 deposition experiments.

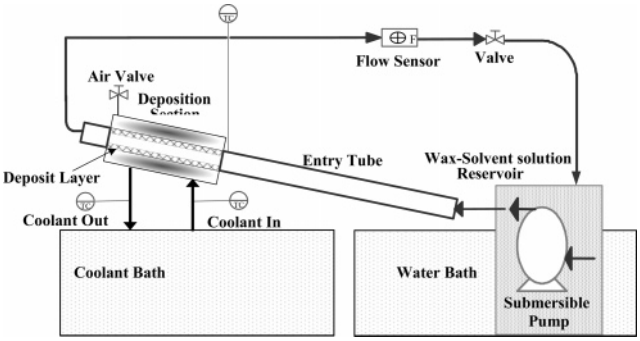

Figure 4. Schematic of the bench-scale flow-loop apparatus for turbulent flow deposition experiments.

All of the deposit samples collected in this study, under turbulent flow, were observed to be quite "firm" and "hard", in contrast to the "soft" and "mushy" deposit samples under laminar flow, as observed by Parthasarathi and Mehrotra.[13] The deposit-layer thickness was also generally much smaller than that reported in previous studies under laminar flow.[1,13]

Design of Experiments. After the completion of approximately 30 preliminary screening experiments, a total of 96 experiments were performed in this investigation according to a factorial design of experiments summarized in Table 2. The experimental program included all of the variables that are known to affect the deposition process, i.e., the composition of the wax−solvent mixture, the inlet temperature of the wax−solvent mixture (T_{hi}), the inlet temperature of the coolant (T_{ci}), and the Reynolds number of the wax−solvent mixture (Re). The range of T_{hi} was from (WAT + 5 °C) to (WAT + 10 °C). The range of T_{ci} was from (WAT − 10 °C) to (WAT − 30 °C). The flow rate of the wax−solvent mixtures was varied over 0.50−1.25 L/s (corresponding to 10 000 < Re < 31 000), while a constant coolant flow rate of 0.0259 L/s was used in all experiments. Each experiment was run for 1 h, and one experiment for every four experiments was repeated to check repeatability. From these 18 repeated experiments, the average variability in the deposit mass was estimated to be ±5.7%.[31] In addition, six extended experiments were conducted with the 15 mass % wax−solvent mixture over 2, 4, and 8 h of deposition time at the highest and lowest Reynolds numbers with T_h = (WAT + 10 °C) and T_c = (WAT − 30 °C). Further details of the experimental program have been provided by Fong.[31]

Estimation of h_h and h_c. Solving the four equalities in eq 3 required estimates for the two heat-transfer coefficients, h_h and h_c. These were obtained through a series of calibration heat-transfer experiments performed with the wax−solvent mixtures held at temperatures higher than WAT, i.e., T_h, T_c > WAT, such that there was no deposition. These calibration experiments were performed at the same coolant rate of 0.0259 L/s (as in the deposition experiments); hence, h_c was assumed to be constant. Ignoring any variation in the properties of wax−solvent mixtures over the relatively small temperature range, it was assumed that $h_h \propto Re^{\alpha}$. With these assumptions, eq 2 for the nondepositing calibration

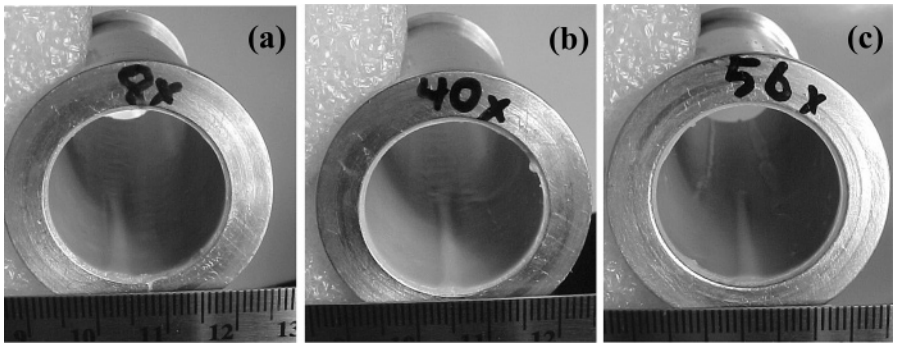

Figure 5. Photographs of the deposition tube showing the "speed bump", following experiments at T_h = (WAT + 5 °C) and T_c = (WAT − 20 °C): (a) 7 mass %, (b) 10 mass %, and (c) 15 mass %.

Table 2. Design of Experiments for Investigating the Deposition from Parowax−Norpar13 Mixtures

variable	number of levels	values of each variable tested
wax concentration (mass %)	3	7, 10, and 15
inlet temperature of the wax−solvent mixture (T_{hi}) (°C)	3	WAT + 5, WAT + 7.5, and WAT + 10
inlet temperature of the coolant (T_{ci}) (°C)	3	WAT − 10, WAT − 20, and WAT − 30
Reynolds number of the wax−solvent mixture (Re)	4 (plus 1 repeat)	10 000 < Re < 31 000
time for deposition (h)		
normal experiments	1	1 h
extended experiments	3	2, 4, and 8 h (for 15 mass % only) at T_h = WAT + 10, T_c = WAT − 30, and Re = 11 400 and 27 600

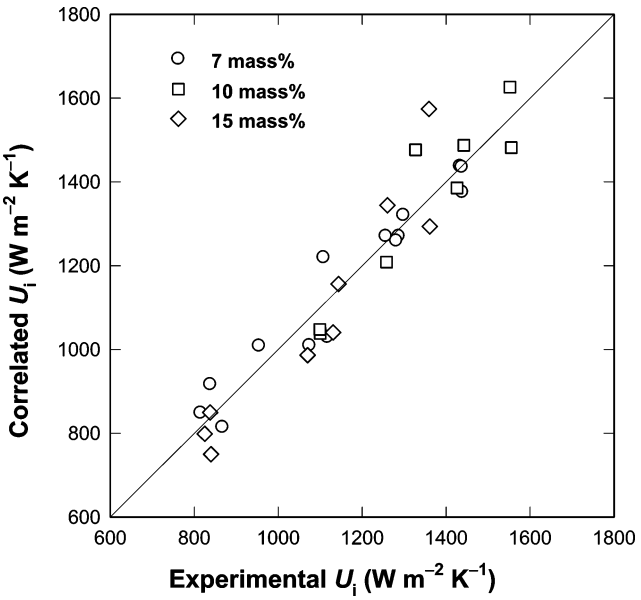

Figure 6. Comparison of the experimental and correlated overall heat-transfer coefficient, U_i, for wax−solvent mixtures (experiments performed under nondepositing conditions).

experiments was simplified as follows:

$$U_i = (\beta \mathrm{Re}^{-\alpha} + \gamma)^{-1} \tag{11}$$

The calibration experiments were carried out for all three wax−solvent mixtures listed in Table 2. Data for the average specific heat capacity, C_c, and the density of water were obtained from Perry's Handbook.[33] The experimental U_i was obtained from eq 1. From a regression analysis with eq 11, using all of the data, α and γ were estimated to be 0.85 and 0.0003, respectively. The optimum values of β for 7, 10, and 15 mass % wax−solvent mixtures were 1.790, 1.613, and 1.905, respectively. With $\gamma = 0.0003$ and k_m = 237.8 W m^{-1} K^{-1}, h_c was estimated to be 2700 W m^{-2} K^{-1}. Depending upon the flow rate (or Re) of wax−solvent mixtures, h_h varied from approximately 1400 to 3600 W m^{-2} K^{-1}.

A comparison of the experimental and correlated U_i for all three wax−solvent mixtures is shown in Figure 6. The average relative deviations between the experimental and calculated U_i were 4.2, 3.9, and 7.2% for 7, 10, and 15 mass % wax−solvent mixtures, respectively. As shown in Figure 1, at $x_d/r_i > 0.01-0.02$, the deposit offered the dominant thermal resistance; hence, the deposition calculations were not affected significantly because of an uncertainty in h_h or h_c.

Deposit Density. The deposit density is expected to depend upon its solid-phase content, compositions of the liquid and solid phases, Reynolds number, and the deposition time. As explained later, these measurements were needed for estimating the average deposit-layer thickness, x_d, as well as for relating the deposit density to the Reynolds number and the average temperature. The deposit samples used in these measurements were from all of the 1 h experiments performed at T_h = (WAT + 7.5 °C) and T_c = (WAT − 20 °C). The average density of deposit samples was measured using a 25 mL glass pycnometer at several temperatures below the respective WAT. The measured deposit densities for each wax−solvent mixture were fitted to the following correlation:

$$\rho_d = d_1 + d_2 \mathrm{Re}^{-1} + d_3(\mathrm{WAT} - T) \tag{12}$$

where T denotes the average deposit temperature. Regression constants d_1, d_2, and d_3 in eq 12 are listed in Table 3. Figure 7 shows the effects of the Reynolds number and temperature on the density of deposit samples obtained from the 10 mass % wax−solvent mixture.

The extent of deposition was expressed as the mass of the deposit per unit inside tube surface area, Ω, which is related to the deposit-layer thickness, x_d, and the deposit density, ρ_d, as follows:

$$\Omega = \rho_d[\{r_i^2 - (r_i - x_d)^2\}/2r_i] \tag{13}$$

For all of the deposition experiments performed in this study, x_d varied from about 0.1 mm ($\Omega \approx 0.079$ kg m^{-2}) to about 0.7 mm

(33) Perry, R. H.; Green, D. W. *Perry's Chemical Engineers' Handbook*; McGraw-Hill: New York, 1997.

Table 3. Correlation of the Average Deposit Density with Reynolds Number and Average Temperature of the Deposition (Applicable at Temperatures Lower than the Respective WAT); Deposit Samples from 1 h Experiments at T_h = (WAT + 7.5 °C) and T_c = (WAT − 20 °C)

	constants in deposit density correlation, eq 11				
wax concentration	d_1	$d_2 \times 10^{-5}$	d_3	R^2	AAD (%)[a]
7 mass %	788.1 ± 2.3	−3.57 ± 0.40	0.785 ± 0.119	0.91	0.22
10 mass %	797.7 ± 1.5	−4.30 ± 0.22	0.860 ± 0.064	0.98	0.16
15 mass %	818.0 ± 8.2	−6.83 ± 1.15	1.783 ± 0.300	0.86	0.93

[a] AAD = $1/n\sum^n$[|calculated − experimental|/experimental].

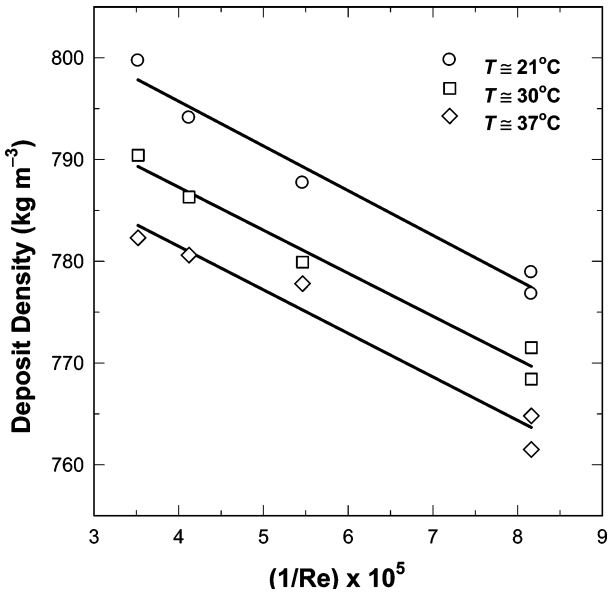

Figure 7. Variation of the deposit density with temperature and the inverse of the Reynolds number [deposit samples from 1 h experiments with 10 mass % wax−solvent mixtures at T_h = (WAT + 7.5 °C) and T_c = (WAT − 20 °C)].

($\Omega \approx 0.53$ kg m^{-2}). Thus, for the 2.5 cm diameter deposition tube, the relative deposit thickness, x_d/r_i, varied from about 0.008 to 0.056. It is noted that the deposit-layer thicknesses in this study were much smaller than those under laminar flow of similar wax−solvent mixtures.[1,13]

Results and Discussion

Results from about 100 deposition experiments are presented and discussed in three subsections. Detailed results for all of the experiments have been reported by Fong.[31]

Section A deals with the measurement of deposit-layer mass from 1 h experiments performed with three wax−solvent mixtures at different temperatures of the wax−solvent mixture (hot) and water (coolant) streams and Reynolds numbers of wax−solvent mixtures. The results are analyzed with eqs 1 and 3 to predict the liquid−deposit interface temperature, T_d, and the average deposit thermal conductivity, k_d. Also, included in section A are the results for the wax content in the deposit samples. Section B presents the results from extended experiments, which were performed to study the changes in the deposit mass and composition with an increased deposition time. Section C presents the GC analyses on deposit samples, collected from experiments in sections A and B, to highlight the changes in carbon-number distributions caused by a variation in the composition and Reynolds number of wax−solvent mixtures as well as the deposition time.

A. Deposit Mass and Properties, 1 h Deposition Experiments. A large number of preliminary deposition experiments indicated that the thermal steady state was attained within 20−30 min.[31] The data for the gain in the coolant temperature ($T_{co} - T_{ci}$) are plotted against time in Figure 8 for the experiments at T_h = (WAT + 10 °C) and T_c = (WAT − 30 °C) for all three wax−solvent mixtures at four Reynolds numbers. In all experiments, ($T_{co} - T_{ci}$) was high initially but decreased rapidly to about 1−2 °C within about 5−10 min and the thermal steady state was reached in about 20−30 min. The temperature profiles in Figure 8 are similar to those reported in a previous deposition study under laminar flow,[1] which also showed the deposition process to be relatively fast, requiring less than 30 min to reach the thermal steady state.

The temperature profiles in Figure 8 also show that ($T_{co} - T_{ci}$) is larger at a higher Reynolds number of the wax−solvent mixture. This is attributed mainly to a decrease in the convective thermal resistance, R_h, and a smaller deposit-layer thickness at higher Reynolds numbers. As shown in eq 1, ($T_{co} - T_{ci}$) is directly proportional to the rate of heat transfer. Thus, an increase in the Reynolds number results in a higher rate of heat transfer at the steady state.

Estimation of T_d and k_d. All of the steady-state data were analyzed using eqs 1 and 3, and the four heat-flux equalities in eq 3 were solved to obtain T_{wi}, T_{wo}, T_d, and k_d. For each set of steady-state data, the experimental T_c was used to calculate T_{wo}, which was used to calculate T_{wi}. Next, the experimental T_h was used to calculate T_d, which was then used to calculate the average thermal conductivity of the deposit, k_d. Note that the ratio $r_i/(r_i - x_d)$ in the first two equalities of eq 3 can be written as $(1 - x_d/r_i)^{-1}$. With $x_d/r_i \ll 1$, T_d estimated from the first equality of eq 1 was less sensitive to x_d. However, the second equality for the heat flux through the deposit layer in eq 3 contains T_d and k_d along with x_d, making the calculated k_d more sensitive to x_d. This is because, even though the term $(1 - x_d/r_i)$ remained close to unity for most experiments, the term $-\ln(1 - x_d/r_i)$ in the second equality of eq 3 varied with x_d/r_i. That is, an experimental uncertainty in x_d caused a relatively larger variation in the estimated k_d than T_d.

For each of the three wax−solvent mixtures, the calculated T_d and k_d did not indicate any trend with other variables.[31] Average values of the liquid−deposit interface temperature, T_d, and the deposit thermal conductivity, k_d, are reported in Table 4. For all three wax−solvent mixtures, T_d is close to the experimentally measured WAT. This observation of $T_d \approx$ WAT was also noted in the previous experimental deposition studies under laminar flow.[1,13]

The average deposit thermal conductivities for 7, 10, and 15 mass % wax−solvent mixtures in Table 4 are nearly the same, i.e., 0.34−0.36 W m^{-1} K^{-1}. The average k_d of 0.35 W m^{-1} K^{-1} is between those of Norpar13 (k = 0.14 W m^{-1} K^{-1})[13] and solid *n*-eicosane (0.42 W m^{-1} K^{-1}), reported by Stryker and Sparrow.[34] The k_d values in Table 4 are higher than those reported for deposits under laminar flow.[1,13] The higher k_d values could be attributed to the higher wax content in the deposit under turbulent flow.

Effects of Re, T_h, and T_c. These three quantities have been

(34) Stryker, P. C.; Sparrow, E. M. Application of a Spherical Thermal Conductivity Cell to Solid *n*-Eicosane Paraffin. *Int. J. Heat Mass Transfer* **1990**, *33*, 1781.

Table 4. Liquid−Deposit Interface Temperature (T_d) and Average Deposit Thermal Conductivity (k_d) Estimated from All Deposition Heat-Transfer Data

	WAT (°C)		
Parowax−Norpar13 mixture	measured (visual)	estimated (T_d)	average estimated thermal conductivity of the deposit, k_d (W m^{-1} K^{-1})
7 mass %	36−37	37.7 ± 1.4	0.36 ± 0.08
10 mass %	38−39	40.9 ± 1.4	0.34 ± 0.07
15 mass %	41−42	42.8 ± 1.4	0.36 ± 0.08
15 mass % (extended experiments)	41−42	42.9 ± 0.8	0.37 ± 0.06

shown to affect the mass of deposits.[1,13] As mentioned previously, the deposit mass was expressed on the basis of a unit deposition area, Ω, by use of eq 13 with the deposit density estimated from eq 12 at the average deposit temperature, $0.5(T_d + T_{wi})$.

It has been shown that the overall temperature difference ($T_h - T_c$) is not correlated to the extent of deposition.[13] The effects of T_h and T_c need to be evaluated in relation to the WAT of each wax−solvent mixture, i.e., in terms of (T_h − WAT) and (WAT − T_c). The results for all three wax−solvent mixtures indicated that the deposit mass was higher for a lower T_h or a lower T_c. That is, the deposit mass was found to be higher for a lower (T_h − WAT) or a higher (WAT − T_c).[31] Similar observations were also reported from the deposition studies under laminar flow,[1,13] as well as the predictions from a mathematical model for the deposition process.[30]

Figure 9 shows the variation of Ω as a function of the Reynolds number, Re, for all three wax−solvent mixture concentrations. The values of Ω in Figure 9 are much smaller than those reported for laminar flow cases,[1,13] which indicate the extent of deposition under turbulent flow to be considerably less than that under laminar flow.

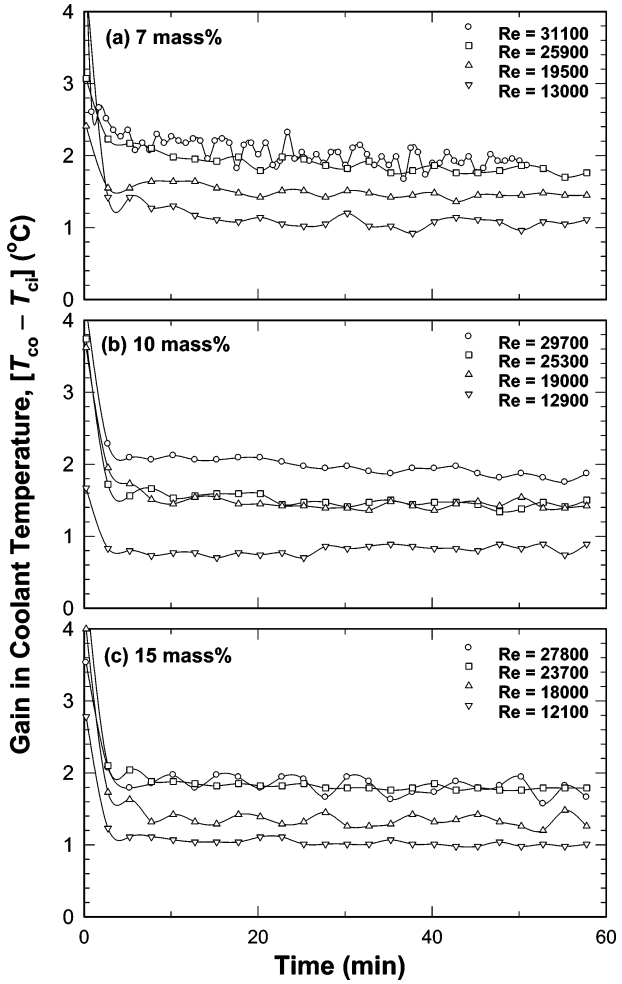

Figure 8. Approach to the thermal steady state during deposition evidenced by the difference in coolant temperatures in 1 h experiments with different wax−solvent mixtures at T_h = (WAT + 10 °C) and T_c = (WAT − 30 °C): (a) 7 mass %, (b) 10 mass %, and (c) 15 mass %.

Each set of symbols in plots a−c of Figure 9 represent the experimental deposit mass obtained with the same values of T_h and T_c. Thus, for constants T_h and T_c, Ω is seen to decrease linearly with an increase in the logarithm of Re. Because $h_h \propto Re^{0.85}$, an increase in Re causes a corresponding increase in h_h and a lower convective thermal resistance, R_h. For the same T_h and T_c, a decrease in R_h translates into a reduction in the deposit thermal resistance, R_d, which implies a decrease in the deposit-layer thickness and consequently a lower deposit mass or Ω. The overall effect of these changes is that the rate of heat transfer is higher at higher Re because of a lower convective thermal resistance as well as a lower conductive thermal resistance offered by the deposit layer.

Fractional Thermal Resistance of the Deposit, θ_d. Figure 10 presents all of the deposit mass data, for the three wax−solvent mixtures at different T_h, T_c, and Re, relating Ω to the fractional thermal resistance offered by the deposit layer, θ_d. The smooth curves represent the predictions from steady-state heat-transfer calculations described previously for the 10 mass % wax−solvent mixture at the indicated values of the deposit thermal conductivity, k_d.

Despite the scatter in Figure 10, the trend in the data is represented adequately by the predicted curve. The agreement between experimental data and predictions suggests that the fractional thermal resistance of the deposit, which is also equal to the fractional temperature drop across the deposit layer, is an important parameter for determining the amount of deposition. For a given Ω or deposit-layer thickness, the results in Figure 10 indicate that a higher k_d would correspond to a lower θ_d. On the other hand, for the same fractional thermal resistance offered by the deposit layer, an increase in k_d would lead to a higher Ω and, consequently, a larger deposit-layer thickness. The relationship between Ω and θ_d in Figure 10 is similar to those shown in previous studies under laminar flow,[1,13] and it provides further support for the deposition to be a thermally driven process.

Deposit Wax Content. The wax content of the deposit was estimated from its GC analysis. The detailed GC results related to changes in the composition of the deposit are presented and discussed later in section C.

Because of the gel-like characteristics of the deposit, it was not possible to separate the liquid phase from the solid phase, while retaining the deposit at the experimental temperature gradient and shear stress. The GC analyses, therefore, gave the average bulk composition of the deposit in terms of the mass fractions of *n*-alkanes ranging from C_5 to C_{50}.[31] Because all carbon numbers less than 19 belonged to the solvent (Norpar13) and those higher than 19 belonged to the wax, the sum of mass fractions of C_{20}^+ constituents was taken to be the wax content of the deposit. The deposit wax content was defined as $\sum_{i=20}^{50}(w_d)_i$, where $(w_d)_i$ is the mass fraction of the *i*th *n*-alkane.

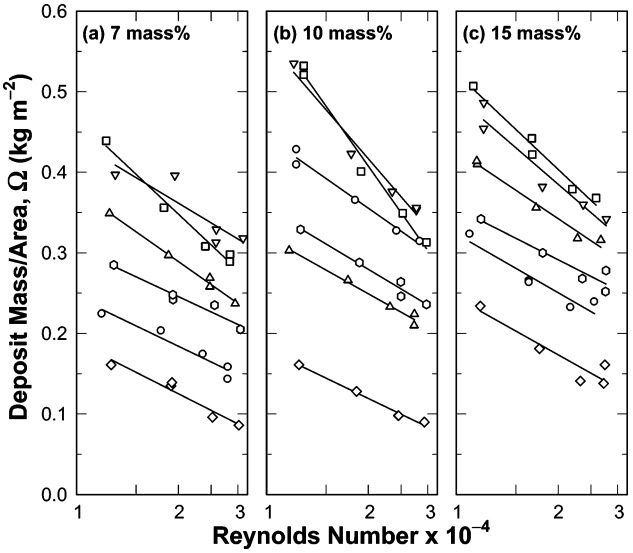

Figure 9. Effect of the Reynolds number, Re, on the deposit mass per unit area, Ω, for 7, 10, and 15 mass % wax−solvent mixtures.

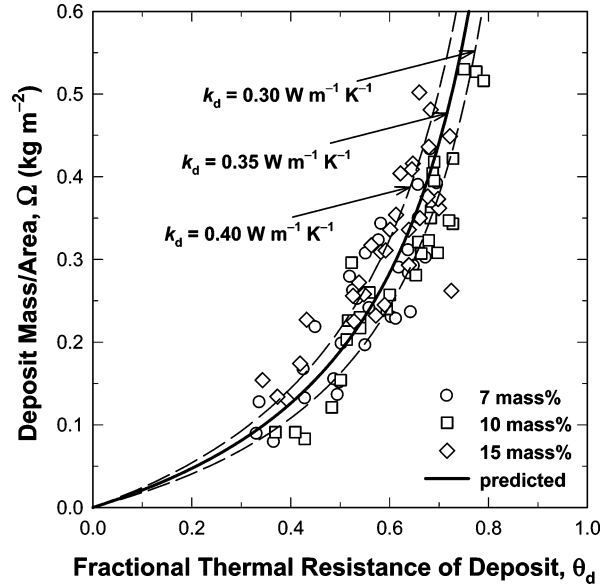

Figure 10. Dependence of the deposit mass per unit area, Ω, on the fractional deposit-layer thermal resistance, θ_d, for all deposition experiments.

It is important to point out that the deposit wax content does not correspond directly to the fraction of the solid phase because the wax content is based on the bulk analysis that would include C_{20}^+ constituents in the solid phase as well as in the liquid phase trapped within the deposit.

Figure 11 shows the effect of the Reynolds number on the deposit wax content for experiments with all three wax−solvent mixtures. All of these experiments were performed at T_{hi} = (WAT + 10 °C) and T_{ci} = (WAT − 30 °C). The deposit wax content is seen to increase with an increase in Re and also with an increase in the concentration of wax in the wax−solvent mixture.

There are two possible explanations for the increase in the deposit wax content with Re. It could be explained in terms of the counter diffusion of lighter and heavier constituents within the deposit, as proposed in a number of studies.[10−12] Another possible explanation could be in terms of the effect of shear stress caused by the flowing wax−solvent mixture during the formation of the deposit layer, which would "squeeze out" the

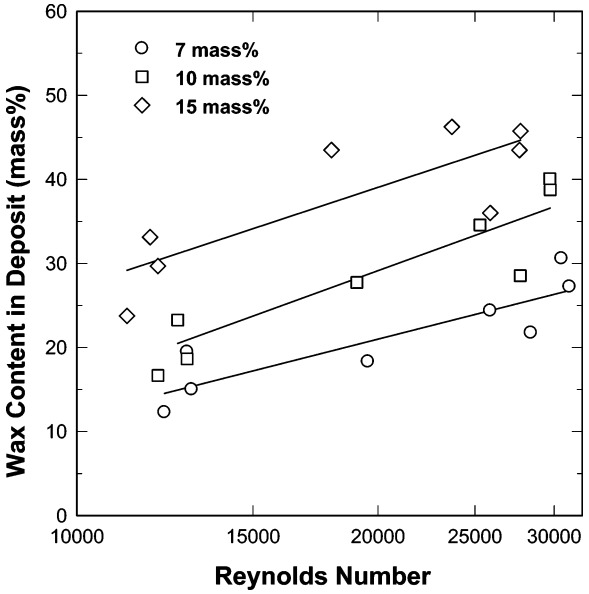

Figure 11. Effect of the Reynolds number, Re, on the deposit wax content for 7, 10, and 15 mass % wax−solvent mixtures.

liquid fraction in the deposition process, as proposed recently.[35] An increase in the Reynolds number will cause a higher shear stress at the liquid−deposit interface, which could lead to an increase in the squeezing out of the liquid fraction from the deposit. With an increased squeezing out of the liquid fraction, the concentration of C_{20}^- *n*-alkanes would decrease, resulting in a higher deposit wax content.

Deposit Wax-Enrichment Ratio, Φ. To compare the wax content in deposit samples from different wax−solvent mixtures quantitatively, a wax-enrichment ratio, Φ, was defined, which compares the wax content of the deposit with that in the wax−solvent mixture, i.e.,

$$\Phi = \frac{\sum_{i=20}^{50} (w_d)_i}{\sum_{i=20}^{50} (w_h)_i} \tag{14}$$

where $(w_h)_i$ denotes the mass fraction of the *i*th C_{20}^+ component in the wax−solvent mixture. All of the data shown in Figure 11 have been replotted in Figure 12, which shows an inverse relationship between Φ and Ω. Also plotted in Figure 12 are similar results obtained under laminar flow.[13] Note that the Ω values obtained under laminar flow are much higher than those obtained in this study under turbulent flow. Also, some of the turbulent flow experiments with the 7 and 10 mass % wax−solvent mixtures gave high values of Φ. The trends shown by both sets of data suggest that a higher deposit mass corresponds to a lower wax-enrichment ratio or a higher liquid-phase content. That is, a thicker deposit formed under a lower Re, a lower (T_h − WAT), and/or a higher (WAT − T_c) is expected to be "softer" or more liquid-like and vice versa.

B. Effect of the Deposition Time, Extended Experiments. Two sets of extended experiments were performed under turbulent flow to study the effect of longer deposition times on the deposition process and changes in the deposit characteristics

(35) Mehrotra, A. K.; Bhat, N. V. Modeling the Effect of Shear Stress on Deposition from "Waxy" Mixtures under Laminar Flow with Heat Transfer. *Energy Fuels* **2006**, manuscript in press.

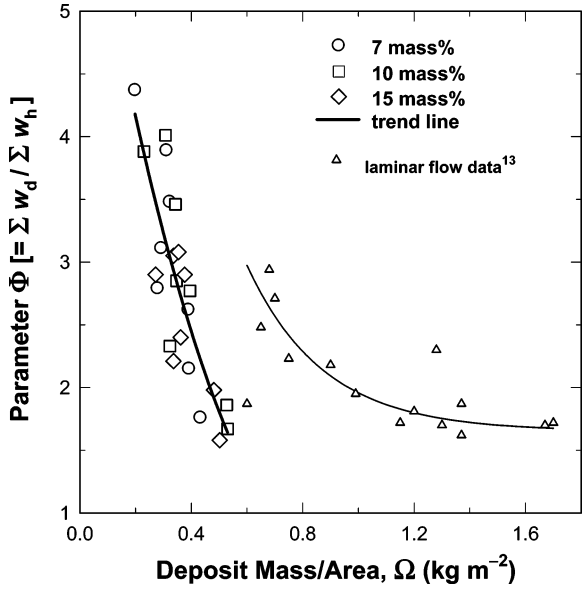

Figure 12. Variation of parameter Φ with Ω for 7, 10, and 15 mass % wax−solvent mixtures and comparison with the laminar flow data of Parthasarathi and Mehrotra.[13]

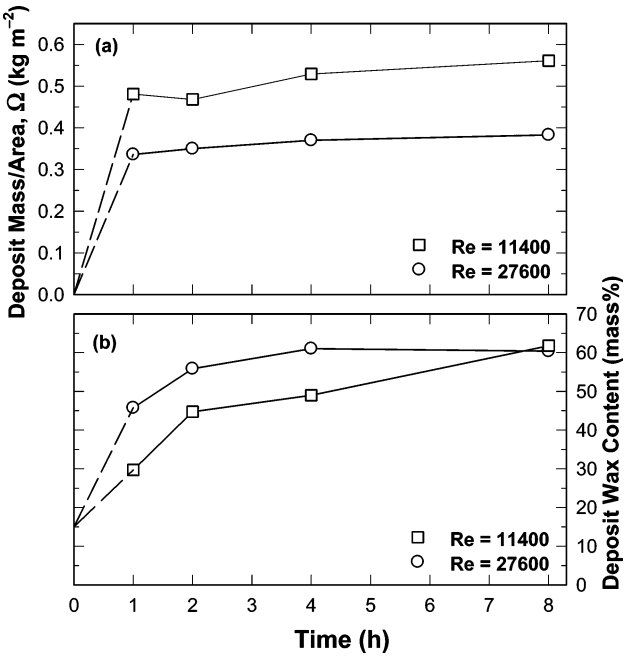

Figure 13. Variation of the deposit mass and wax composition with time for 15 mass % wax−solvent mixtures at T_h = (WAT + 10 °C) and T_c = (WAT − 30 °C): (a) deposit mass and (b) deposit wax composition.

with time, referred to as the "deposit aging." All of these extended experiments were performed with the 15 mass % wax−solvent mixture at Re = 11 400 and 27 600 with T_h = (WAT + 10 °C) and T_c = (WAT − 30 °C). The results for Ω and the deposit wax content at the two Reynolds numbers are plotted against time in plots a and b of Figure 13, respectively. Figure 13 shows that much of the deposition occurred within 1 h and the deposit mass increased somewhat from 1 to 8 h. The increase in the deposit mass with time is relatively larger at the lower Re compared to that at the higher Re. Even though the deposit mass did not increase as much, the deposit wax content increased quite significantly from 1 to 8 h. The increase in the deposit wax content with time is relatively slower at the lower Re, reaching its maximum value of about 60 mass % for the 8 h experiment. The deposit wax content at the higher Re reached its ultimate value of about 60 mass % in 2−4 h. Note that the deposit wax content of 60 mass % for the 15 mass % wax−solvent mixture corresponds to Φ = 4, which is a high wax-enrichment ratio.

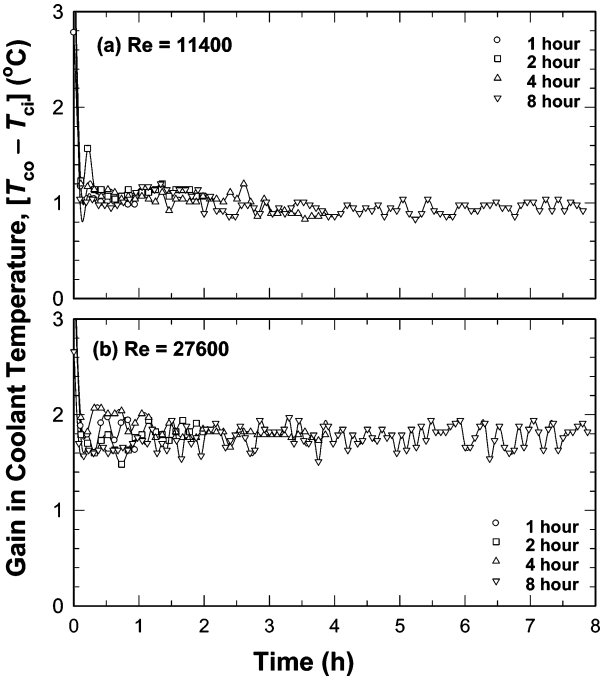

Figure 14. Approach to the thermal steady state during extended deposition experiments with 15 mass % wax−solvent mixtures at T_h = (WAT + 10 °C) and T_c = (WAT − 30 °C): (a) Re = 12 100, and (b) Re = 27 800.

The average values of the liquid−deposit interface temperature, T_d, and the deposit thermal conductivity, k_d, for the extended experiments are listed in Table 4. The average T_d and k_d from the extended experiments are nearly the same as those for the 1 h experiments.

To explore the effects of an increase in Ω and the deposit wax content (or Φ) on the rate of heat transfer, the data for $(T_{co} - T_{ci})$ from all extended experiments at both Re are plotted against time in Figure 14. Note that $(T_{co} - T_{ci})$ for the experiments at Re = 27 600 is higher than that at Re = 11 400, which indicates a higher rate of heat transfer at the higher Re because of lower thermal resistances, R_h and R_d. At each Reynolds number, all four temperature profiles show the same steady-state value of $(T_{co} - T_{ci})$, which indicates that the rate of heat transfer did not change appreciably between 1 and 8 h. That is, an increase in Ω and the deposit wax content (or Φ) from 1 and 8 h, as seen in Figure 13, did not alter the thermal steady state, which was reached within the first 20−30 min.

As pointed out previously, the deposit thermal resistance, R_d, depends upon the magnitudes of k_d and x_d but not directly on its mass (or Ω). The second equality in eq 3, $q/A_i = [k_d(T_d - T_{wi})]/[r_i \ln\{r_i/(r_i - x_d)\}]$, indicates that x_d will vary only with a change in q, T_d, or k_d. Considering that q, T_d, and k_d did not vary between the 1 h and extended experiments, one possible explanation for the observed increase in Ω from 1 to 8 h, in Figure 13a, is that an increase in Ω corresponds to an increase in Φ, resulting in an increase in the deposit density, ρ_d. That is, the increase in Ω with time, as observed in Figure 13a, is possibly due to an increase in ρ_d. In eq 13, Ω is directly proportional to ρ_d. Hence, if both Ω and ρ_d were to increase by the same extent because of wax enrichment, the average deposit thickness, x_d, could remain constant, which would cause the

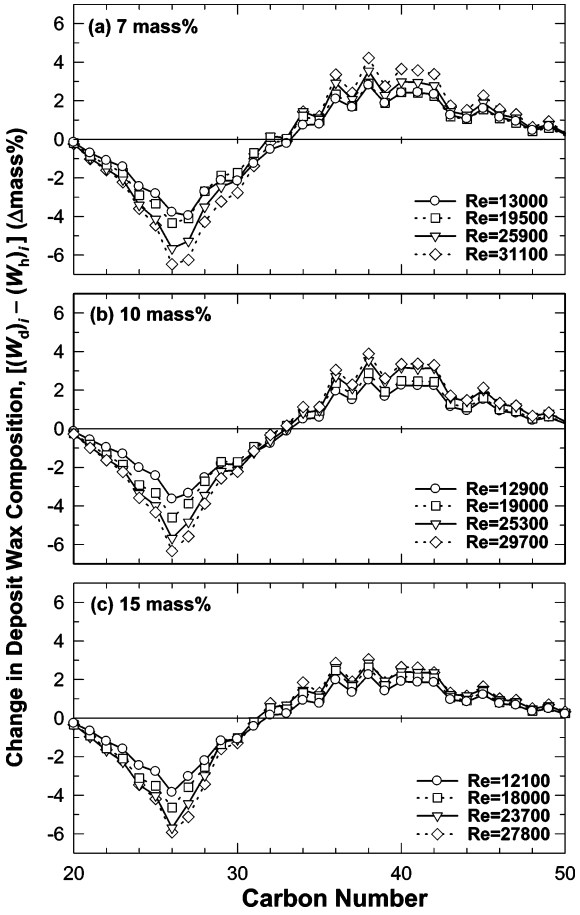

Figure 15. Effect of the Reynolds number, Re, on the change in the deposit composition for different wax−solvent mixtures at T_h = (WAT + 10 °C) and T_c = (WAT − 30 °C): (a) 7 mass %, (b) 10 mass %, and (c) 15 mass %.

deposit thermal resistance, R_d, and the rate of heat transfer, q, to remain unchanged with time in the extended experiments. This will yield the same thermal steady state during the extended experiments, as indicated by the results in Figure 14. The above analysis based on the heat-transfer considerations could be verified further in future studies.

C. Changes in the Carbon-Number Distribution in Deposit Samples. In section A, GC analyses were used for estimating the deposit wax content. The results presented in this section are for the changes in the carbon-number distribution in deposit samples collected from the same 1 h and extended experiments. All of the GC analyses on the 1 h deposit samples were from the experiments performed at T_h = (WAT + 10 °C) and T_c = (WAT − 30 °C). As mentioned previously, the 2, 4, and 8 h deposit samples were from the extended experiments performed at Re = 11 400 and 27 600 with the 15 mass % wax−solvent mixture at T_h = (WAT + 10 °C) and T_c = (WAT − 30 °C).

To highlight changes in the carbon-number distribution of deposit samples, the mass fractions of C_{20}−C_{50} *n*-alkanes were normalized on a solvent-free basis. The normalized mass fractions of *n*-alkane with the *i*th carbon number in the deposit, $(W_d)_i$, and in the wax−solvent mixture, $(W_h)_i$, were calculated as follows:

$$(W_d)_i = \frac{(w_d)_i}{\sum_{j=20}^{50}(w_d)_j} \qquad (W_h)_i = \frac{(w_h)_i}{\sum_{j=20}^{50}(w_h)_j} \qquad (15)$$

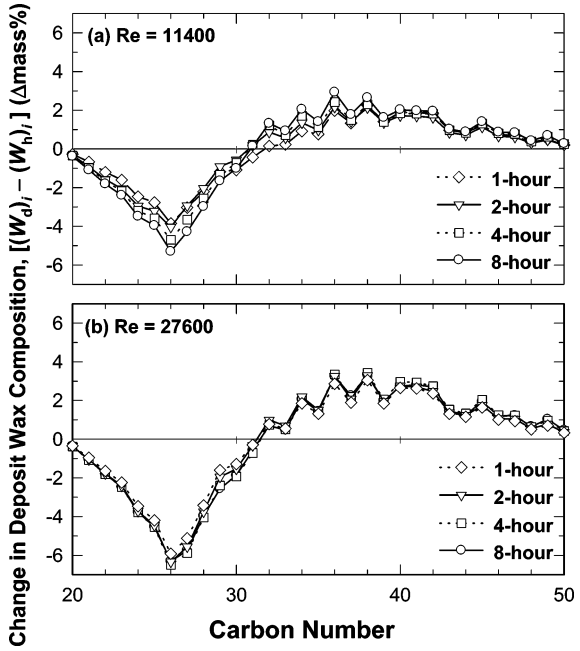

Figure 16. Changes in the deposit composition with time for extended experiments at two Reynolds numbers, Re, with 15 mass % wax−solvent mixtures at T_h = (WAT + 10 °C) and T_c = (WAT − 30 °C): (a) Re = 11 400, and (b) Re = 27 600.

The difference between the above two normalized mass fractions $[(W_d)_i - (W_h)_i]$ represented the change in the composition of *n*-alkane with the *i*th carbon number. This difference for each carbon number was expressed as a deviation or Δmass %.

Composition Changes in Deposit Samples from 1 h Experiments. Figure 15 shows the changes in the deposit wax composition, as deviations, for *n*-alkanes ranging from C_{20} to C_{50} for the 1 h deposit samples from all three wax−solvent mixtures at the four Reynolds numbers. As mentioned previously, the data in Figure 15 are for deposit samples collected at T_h = (WAT + 10 °C) and T_c = (WAT − 30 °C). All of the curves in Figure 15 have a sharp minimum at C_{26} and a flat maximum at about C_{36}−C_{38}. The deviations are close to 0 for C_{20}, C_{32}, and C_{50}. In all cases, the deviations are negative by as much as −6 to −7 Δmass % for carbon numbers from C_{20} to C_{31} and positive by up to about +4 Δmass % for carbon numbers from C_{33} to C_{50}. More importantly, all of the curves for the three wax−solvent mixtures are qualitatively and quantitatively similar, which suggests that the deviations in carbon-number distributions are independent of the mixture composition (provided that T_h and T_c differ by the same amount from their respective WAT).

Figure 15 shows that an increase in Re causes a greater change in the carbon-number distribution for all three wax−solvent mixtures. In all cases, at the lowest Reynolds number of 12 000−13 000, the minimum and maximum deviations are about −4 and +2 Δmass %, respectively; however, at the highest Reynolds number of 28 000−31 000, the respective values are much larger at −6 to −7 and +4 Δmass %. The results in Figure 15 together with those in Figure 11 show that, for a given wax−solvent mixture at the same T_h and T_c (relative to WAT), an increase in Re yields a deposit that has a higher wax content as well as increased mass fractions of *n*-alkanes heavier than C_{32} and decreased mass fractions of *n*-alkanes lighter than C_{32}. In summary, Re has a significant effect on the deposit wax content and composition.

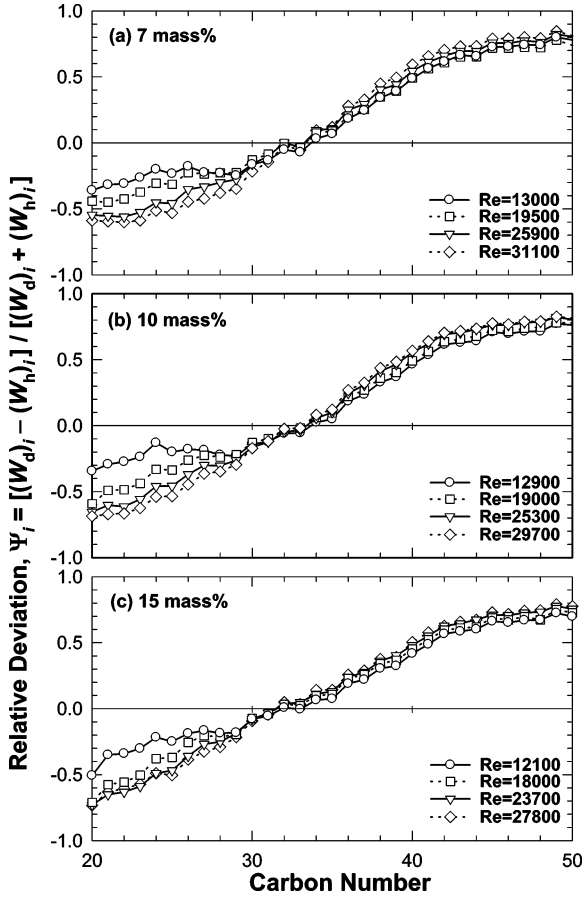

Figure 17. Effect of the Reynolds number, Re, on the relative change in the deposit composition, Ψ_i, for different wax−solvent mixtures at T_h = (WAT + 10 °C) and T_c = (WAT − 30 °C): (a) 7 mass %, (b) 10 mass %, and (c) 15 mass %.

Composition Changes in Deposit Samples from Extended Experiments. The two plots in Figure 16 show the changes in the deposit wax composition at Re = 11 400 and 27 600. As mentioned previously, all of these extended experiments were performed with the 15 mass % wax−solvent mixture at T_h = (WAT + 10 °C) and T_c = (WAT − 30 °C). All of the curves in Figure 16 have the same shape, which is also similar to that in Figure 15c, i.e., a sharp minimum at C_{26} and a flat maximum at about C_{36}−C_{38}. At the lower Re, in Figure 16a, at the shortest deposition time of 1 h, the minimum and maximum deviations are about −4 and +2 Δmass %, respectively; however, at the longest deposition time of 8 h, the corresponding values are much larger at −6 and +3 to +4 Δmass %. It is pointed out that the term "deposit aging" mentioned in the literature relates to this change in the deposit composition with time. Thus, the deposit aging is evident in the results at the lower Re of 11 400. In Figure 16b, however, the deviations do not change appreciably with time; that is, there is no significant deposit aging evident at the higher Re of 27 600.

Thus, the results in Figure 16 together with those in Figure 13 show that a slight increase in the deposit wax content together with a change in the deposit composition, with time, is seen only at the lower Re. These effects diminish as the Reynolds number is increased.

Relative Change in Deposit Composition. The results in Figures 15 and 16 showed changes in the normalized concentration of *n*-alkanes in the deposit on an absolute basis. The largest deviation corresponding to the minima in all of the carbon-number distributions occurred at C_{26}. The changes in the carbon-number distribution of deposit samples are further evaluated

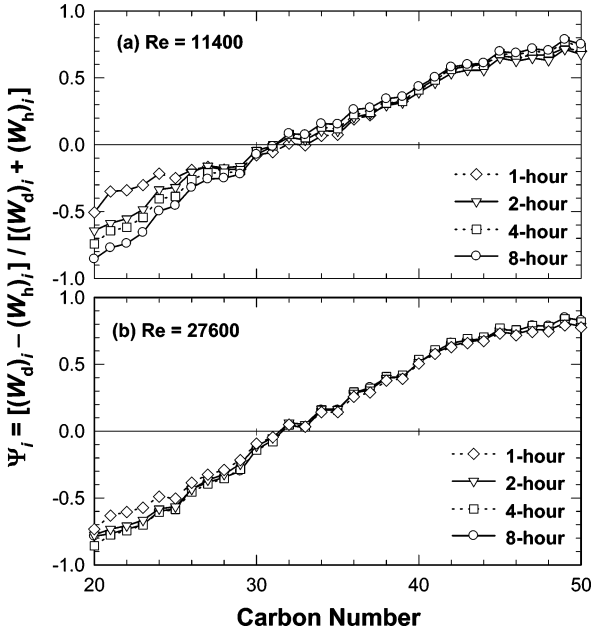

Figure 18. Variation in the relative change in the deposit composition, Ψ_i, with time for extended experiments at two Reynolds numbers, Re, with 15 mass % wax−solvent mixtures at T_h = (WAT + 10 °C) and T_c = (WAT − 30 °C): (a) Re = 11 400, and (b) Re = 27 600.

by defining a relative deviation for the *i*th *n*-alkane, Ψ_i, as follows:

$$\Psi_i = \frac{(W_d)_i - (W_h)_i}{(W_d)_i + (W_h)_i} \tag{16}$$

As explained below, the above definition of relative deviation offers an advantage over its more conventional definition; i.e., relative deviation = $[(W_d)_i - (W_h)_i]/(W_h)_i$. According to eq 16, when $(W_d)_i \gg (W_h)_i$, $\Psi_i \to +1$; when $(W_d)_i \ll (W_h)_i$, $\Psi_i \to -1$; and when $(W_d)_i = (W_h)_i$, $\Psi_i = 0$. Thus, for the entire mass fraction domain, $0 \le (W_d)_i \le 1$, the range for the relative deviation is $-1 \le \Psi_i \le +1$. In other words, with the definition of relative deviation in eq 16, Ψ_i can only vary between −1 and +1. In contrast, for the deposit compositional data in Figures 15 and 16, the conventional definition gave relative deviations from −1 to +10 or higher.[31]

Figure 17 shows the variation of Ψ_i for all of the data included in Figure 15. The trends for relative deviations in Figure 17 are very different from those for the (absolute) deviations in Figure 15. The results in Figure 17 show that the largest relative deviations occur for C_{20} and C_{50}, which are the lightest and heaviest *n*-alkanes in the wax sample, respectively. The lowest and highest numerical values of Ψ_i are about −0.7 (for $i = C_{20}$) and about +0.8 (for $i = C_{50}$), respectively. As expected from the results in Figure 15, $\Psi_i = 0$ for $i = C_{32}$ in all cases. However, the curves in Figure 17 do not show any noticeable characteristic at the carbon numbers corresponding to the minima and maxima in Figure 15.

Thus, the results in Figure 17 indicate that all of the deposit samples were enriched in the heaviest *n*-alkane and depleted in the lightest *n*-alkane. An increase in Re caused a further depletion of the lighter *n*-alkanes in the deposit; however, it did not yield a corresponding further enrichment of the heavier *n*-alkanes.

Similar results for the deposit samples from the extended experiments are shown in Figure 18. At the lower Re = 11 400, Figure 18a shows that the effect of an increased deposition time

on Ψ_i is similar to that for the effect of an increased Re in Figure 17. This suggests that the changes in deposit characteristics associated with "deposit aging" would be similar to those caused by an increased Re over the shorter 1 h deposition time. At the higher Re = 27 600 in Figure 18b, it is noted that the curves for the 2, 4, and 8 h extended experiments overlap for all carbon numbers. This observation, together with the results in Figure 13b, suggests that the "deposit aging" becomes less significant as the Reynolds number is increased.

Conclusions

A bench-scale flow-loop apparatus was developed to investigate the role of heat transfer in deposition from waxy mixtures under turbulent flow conditions. Deposition experiments were performed with three wax concentrations of 7, 10, and 15 mass %, at four levels of the Reynolds number, three levels of the wax−solvent mixture temperature, and three levels of the coolant temperature. Extended experiments, lasting up to 8 h, were performed to study the effect of the deposition time on deposit properties. The deposition data were analyzed with a steady-state heat-transfer model, which indicated the deposition process to be predominantly thermally driven. Similar to previous studies under laminar flow, the deposition process under turbulent flow was found to be relatively fast, requiring less than 30 min to reach the thermal steady state.

For all wax−solvent mixtures, the liquid−deposit interface temperature, T_d, was found to be close to the experimentally measured WAT. The average deposit thermal conductivity was estimated to be 0.35 ± 0.08 W m^{-1} K^{-1}. The deposit density was shown to vary with the average temperature and Re of the deposition experiment.

The extent of deposition under turbulent flow was considerably less than that under laminar flow. An increase in the temperature of the wax−solvent mixture and Re resulted in a decreased deposit mass. An increase in the coolant temperature also yielded a lower deposit mass. That is, the deposit mass was found to be higher for a lower (T_h − WAT) and/or a higher (WAT − T_c). An increase in Re also caused a higher rate of heat transfer at the steady state because of a lower convective thermal resistance as well as a lower conductive thermal resistance of a thinner deposit layer. The deposit mass was related to the fractional thermal resistance of the deposit (or the fractional temperature drop across the deposit layer) at the steady state.

The deposit wax content increased with an increase in Re as well as the wax concentration in the wax−solvent mixture. A parameter, Φ, was defined to describe quantitatively the enrichment of C_{20}^+ *n*-alkanes in the deposit in relation to that in the wax−solvent mixture. The trends in experimental data suggested that a higher deposit mass corresponds to a lower Φ.

Extended experiments were performed to study the "deposit aging" phenomenon. It was shown that much of the deposition took place within 1 h, followed by a small increase in the deposit mass and wax content from 1 to 8 h, particularly at the lower Re. However, the thermal steady state was not altered in these extended experiments beyond 1 h.

The GC analysis of deposit samples showed interesting changes in their carbon-number distributions. An increase in Re yielded a deposit that had a higher wax content as well as increased mass fractions of *n*-alkanes heavier than C_{32} and decreased mass fractions of *n*-alkanes lighter than C_{32}. An increase in the deposition time caused changes in the deposit composition at the lower Re, but such changes were not evident at the higher Re. When compared on a relative basis, an increase in Re caused a further depletion of the lighter *n*-alkanes in the deposit but did not yield a significant enrichment of the heavier *n*-alkanes. An increased deposition time also caused a similar depletion of the lighter *n*-alkanes in the deposit but more so at the lower Re. That is, the deposition results under turbulent flow indicated that the "deposit aging" occurs more rapidly at higher Re.

Acknowledgment. Financial support from the Natural Sciences and Engineering Research Council of Canada (NSERC) and the Department of Chemical and Petroleum Engineering (University of Calgary, Calgary, Alberta, Canada) is gratefully acknowledged. We thank Mr. Nitin Bhat, Ms. Elizabeth Zalewski, Mr. Bernie Then, and Mr. Paul Stanislav for their valuable input, GC analyses, and technical support.

Nomenclature

a_1, a_2, b_1, b_2, c_1, c_2, d_1, d_2, and d_3 = regression constants in eqs 8−10
A_i = inside surface area of the tube or deposition surface area (m^2)
C_c = average specific heat capacity of the coolant (J kg^{-1} K^{-1})
C_h = average specific heat capacity of the wax−solvent (hot) mixture (J kg^{-1} K^{-1})
h_c = heat transfer coefficient for the coolant (W m^{-2} K^{-1})
h_h = heat transfer coefficient for the wax−solvent (hot) mixture (W m^{-2} K^{-1})
k_d = average thermal conductivity of the deposit (W m^{-1} K^{-1})
k_m = thermal conductivity of aluminum (W m^{-1} K^{-1})
L = length of the aluminum tube (m)
$\dot{m}_c$= mass rate of the coolant (kg s^{-1})
$\dot{m}_h$= mass rate of the wax−solvent mixture (kg s^{-1})
q = rate of the heat transfer at the steady state (W)
q_{gain} = rate of the heat gain by the coolant from the surroundings, $<0.01q$ (W)
R^2 = coefficient of determination
R_c = thermal resistance of the coolant (K W^{-1})
R_d = thermal resistance of the deposit layer (K W^{-1})
R_h = thermal resistance of the wax−solvent mixture (K W^{-1})
R_m = thermal resistance of the aluminum tube wall (K W^{-1})
r_i = inside tube radius (m)
r_o = outside tube radius (m)
Re = Reynolds number
T = temperature (°C)
T_c = average temperature of the coolant $\equiv 0.5T_{ci} + 0.5T_{co}$ (°C)
T_{ci} = inlet temperature of the coolant (°C)
T_{co} = outlet temperature of the coolant (°C)
T_d = average temperature at the interface of the deposit and wax−solvent mixture (°C)
T_h = average temperature of the wax−solvent mixture $\equiv 0.5T_{hi} + 0.5T_{ho}$ (°C)
T_{hi} = inlet temperature of the wax−solvent mixture (°C)
T_{ho} = outlet temperature of the wax−solvent mixture (°C)
T_{wi} = temperature at the inside aluminum tube surface (°C)
T_{wo} = temperature at the outside aluminum tube surface (°C)
U_i = overall heat-transfer coefficient based on the deposition tube inside surface area (W m^{-2} K^{-1})
w_d = mass fraction of C_{20}^+ *n*-alkane in the deposit
W_d = normalized (solvent-free) mass fraction of C_{20}^+ *n*-alkane in the deposit
w_h = mass fraction of C_{20}^+ *n*-alkane in the wax−solvent mixture
W_h = normalized (solvent-free) mass fraction of C_{20}^+ *n*-alkane in the wax−solvent mixture
x_d = deposit-layer thickness (m)

Greek Letters

α, β, and γ = empirical constants in eq 11
μ = viscosity of the wax−solvent mixture (Pa s)
ρ = density of the wax−solvent mixture (kg m^{-3})
ρ_d = density of the deposit (kg m^{-3})

θ_c = ratio of the coolant (convective) thermal resistance and total thermal resistance
θ_d = ratio of the deposit (conductive) thermal resistance and total thermal resistance
θ_h = ratio of the wax−solvent mixture (convective) thermal resistance and total thermal resistance
θ_m = ratio of the tube-wall (conductive) thermal resistance and total thermal resistance
Ω = mass of the deposit per unit deposition surface area (kg m^{-2})
Φ = ratio of C_{20}^+ *n*-alkane contents in the deposit and wax−solvent mixture
Ψ_i = relative deviation in the normalized mass fraction of the *i*th *n*-alkane in the deposit (defined in eq 16)

Acronyms

GC = gas chromatograph
WAT = wax appearance temperature (°C)
WDT = wax *dis*appearance temperature (°C)
AAD = average absolute deviation

EF0603784